Mechanical and Control System Development for a Full-scale Planar Motion Spacecraft Simulator

Dario Riccobono[1]
Politecnico di Torino, Torino, Italy, 10129

The main subject of the research described in this paper focuses on the design, development and hardware implementation of some crucial subsystems for a full-scale/mass, air-levitated spacecraft emulator testbed. The subsystems developed involve the Guidance, Navigation and Control system, the Electric Power System, the onboard electronics and the structural frame. The testbed was designed and developed at NASA Jet Propulsion Laboratory, California Institute of Technology, as part of the technology development and validation for a potential future Comet Surface Sample Return mission.

I. Introduction

Return of a sample from the surface of a comet was identified as one of NASA's highest science priorities in the Decadal Survey of the National Research Council published in 2011 [1,2]. Several potential architectures are possible for a Comet Surface Sample Return (CSSR) mission, including lander, harpoon, dart, and Touch-And-Go (TAG) [3,4].

The Jet Propulsion Laboratory (JPL), California Institute of Technology, has developed the BiBlade sampling chain for use in a potential CSSR mission using a TAG architecture. In a TAG mission architecture (Fig. 1) a spacecraft (SC) would maneuver to several meters from the surface of a small body, deploying a sampling tool at the end of a robotic arm. The SC would continue descent to the surface until sample tool contact, then a sample would be quickly acquired. Finally, the SC would thrust away from the surface of the small body. The BiBlade sampling tool is composed by two blades, driven into the comet surface using springs in about 30 ms. The blades can encapsulate up to 500 cm^3 of surface material. The robotic arm would then transfer the sample inside the measurement station, where fiberscopes would carry images of the sample from multiple locations. Pulling back the blades all the way, the sample could be finally deposited in one of the two sample canisters of a Sample Return Capsule (SRC). At this point a second sample could then be acquired. The BiBlade sampler is mechanically simple, acquiring and encapsulating a sample in a fast sampling action. It enables multiple sampling attempts and return of two samples with one sampling tool, making it a minimally complex system for a CSSR mission concept. The sampling chain for CSSR technology was developed and validated to TRL 6.

A full-scale/mass air-levitated SC emulator (SCE) was also designed and fabricated at JPL for integrated validation of TAG sampling chain. The goal was to reproduce the SC operations in a two-dimensional (2D), low-friction plane. The SCE has then three Degrees of Freedom (DoFs) of motion, longitudinal and transversal linear motion, and rotational motion.

In the TAG sampling chain validation test, the SCE approaches the target by means of air thrusters to control its attitude, direction and velocity of motion. Once the sampling tool touches the target, the sampling process is completed in almost 30 ms, then the SCE thrusts away from the target. The target is a small cube with a side of about 30 cm, and it is composed by a wooden box which encapsulates the comet simulant, called Manufactured Porous Ambient Comet Simulant (MPACS). The MPACS is made of Portland cement and pumicite combined and added to water and Varimax foaming agent. The mechanical properties were evaluated measuring density, cone penetration resistance (CPR), uniaxial compressive strength (UCS), shear strength, and porosity [5].

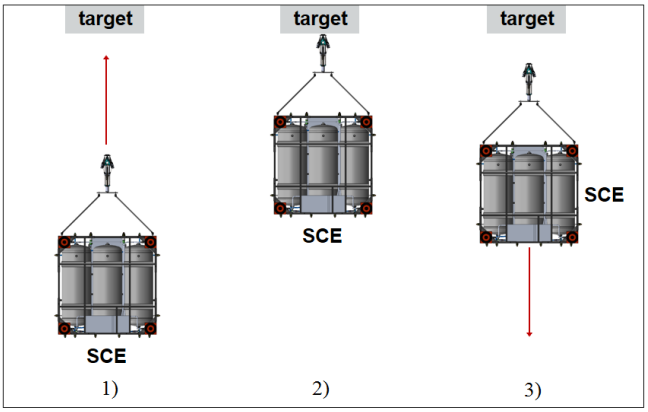

Figure 1. TAG Sampling chain: 1) approaching the target; 2) sampling process; 3) leaving the target.

[1] Ph.D. Candidate in Mechanical Engineering, Department of Mechanical and Aerospace Engineering (DIMEAS), Corso Duca degli Abruzzi 24, 10129 Torino (Italy), not an AIAA member.

II. Spacecraft Emulator Testbed Overview

A. Air-levitation System

The SCE moves and reacts on the 2D plane as if it would be in a microgravity environment. To guarantee such a behavior, a low-friction, 2D system was designed. Air bearings were selected to realize a thin layer of pressurized air between the floor and the SCE so that the friction can be considerably reduced. Having no contact, air bearings avoid standard issues such as friction and lubricant handling. On the other side, they can guarantee high precision positioning and high-speed applications [6].

Tests performed on air bearings from Aerogo Inc., showed high repeatability without loss of efficiency over time with a simple treated concrete floor, giving more repeatability and less restriction on the type of floor [7]. However, some drawbacks were faced due to higher friction and higher air flow rate with respect to other types of air bearings. Even considering these issues, the Aerogo system was selected as main lifting system for the SCE [8]. The Aerogo Inc. company uses a technology that consists in inflating compressed air into the bearing. The working principle is the following; the air bearing plate is directly connected to a torus bag that inflates, touches the floor surface, and raises the load. Once the pressure and the flow rate are sufficient to create an offset between the bearing and the floor, air slowly escapes from the torus bag, creating a thin film 0.08 mm to 0.13 mm thick.

The air bearings are supplied with pressurized air at 6 bar with a flow rate depending on the load that would be lifted. If the air bearings are supplied with a flow rate higher than the amount needed for a defined load, than there is an improvement on performances, especially in terms of friction reduction due to the higher air film thinness achievable. Tests showed a high friction coefficient that, together with an uneven floor, drove the sizing of the propulsion system.

The main components of the air-levitation system are three tanks of 240 gal each, where the pressurized air is stored, the pressure lines and the valves to carry the compressed air to the air bearings.

B. Propulsion System

The SCE required a propulsion system to perform both attitude and trajectory control. Historically, cold gas, bi-propellant and mono-propellant have been used. Cold gas systems are less risky, costly and complex with respect to others. On the other hand, they have the lowest specific impulse and thrust. Pressure and weight were the main guidelines for the propulsion system type selection. Because of safety requirements, the system was developed for low pressures (maximum 13.5 bar). By adopting this solution, the system is also more reliable, and with a less recharge time. For these reasons, the cold gas system architecture was chosen.

Several aspects were considered to select the most suitable propellant. Air was selected for the good specific impulse of around 74 seconds, non-toxicity, non-reactivity, high availability and compatibility with materials [8]. Air can be also easily stored in low pressurized tanks without any specific safety procedure.

The propulsion system has two main purposes.

- Provide the right thrust to overcome friction and keep the SCE's approaching velocity at the desired value.
- Provide transversal and rotational forces to control the SCE's attitude and overcome external disturbances, such as gravity due to not flatness of the floor.

A total of fourteen thrusters were adopted to comply with requirements. Thrusters were oversized to provide 100% more force than required, preventing unexpected events in terms of disturbances [8]. This was done specifically because of the high uncertainty about floor flatness.

The main components of the propulsion system are two tanks of 240 gal each, where the pressurized air is stored at the maximum pressure of 13.5 bar, the pressure lines to carry the compressed air to the valves, and the related nozzles. Instead of having a pressure regulator for each valve, two secondary tanks of 30 gal each were pressurized at the operational pressure of the thrusters. Each secondary tank is connected with a main tank via a pressure regulator in between. This configuration avoids using a pressure regulator for each thruster.

On/off solenoid valves were preferred to flow regulation valves to manage the air flow through the thrusters. In this case, the cost was the main driver. The flow regulation valves enable thrust control by air flow regulation; this is achieved by managing the valve opening through a continuous control. On the other hand, on/off valves cannot regulate the valve opening since there are only two available positions: completely open, and completely closed, controlled via impulsive control (i.e. Pulse-Width-Modulation, PWM). The response time given by the vendor (i.e. Granzow) is about 30 ms, which is acceptable for a good PWM control [8]. Therefore, solenoid valves offer fast and safe switching, high reliability, long service life, good medium compatibility of the materials used, low control power and compact design. The valves selected are normally closed. In case of loss of power, the valves are designed to return in the not energized position, closing the outlet and ensuring a safe response also in case of emergency. The valves selected are rated for about 13.5 bar, according with the maximum pressure of the tanks. Furthermore, since the testbed is completely off-the-grid, the 24 VDC version was selected.

The last component to be considered is the nozzle. This is the main component that allows to fully expand the gas and reach the maximum thrust at the operating pressure. A convergent/divergent nozzle was designed and produced by using a 3D printer to check sizing and performances, then a comparison with an aluminum version was performed. Tests showed that aluminum nozzle does not have any significant improvement in performance. Consequently, 3D printed nozzles were implemented for the low cost and fast production time [8].

C. Mechanical Frame

The mechanical structure hosts and supports the air-levitation system, the propulsion system, the Electric Power System (EPS), and the onboard electronics. The frame is constrained in a cube shape of approximately 2.5 m x 2.5 m x 2.5 m. A three-floors configuration was implemented. The first floor is placed at the bottom level, the second floor at the mid height of the structure, the third floor at the top of the cube. The air-levitation system is placed on the bottom floor to be as near as possible to the air bearings. The propulsion system is placed on the mid floor, whereas the EPS and the onboard electronics are suspended underneath the top floor.

The structure is made of standard 80/20 T-slotted profiles made of 6105-T5 aluminum alloy. Commercial off-the-shelf (COTS) components was selected to reduce costs. Moreover, standard fixtures, nuts, plates, brackets, etc. were adopted. Finite Element Analysis (FEA) was performed to determine the right T-slotted profile size. The load cases considered included motion and lifting. The motion load case considered the loads applied to the mechanical frame in case of testbed hard stop during maximum speed motion. The lifting case considered the loads applied to the structure in case of lifting for repositioning needs when the testbed is not used for tests.

III. Guidance, Navigation, and Control System

A closed-loop Guidance, Navigation, and Control (GNC) system was selected to deals with the management of the SCE's motion, since a control of position and velocity was required. This was achieved by using a feedback loop, which links the control actions to the error between the desired and actual state of the system.

In particular, the GNC system was designed to perform the following duties [9].

- *Navigation*, refers to the determination of the SCE's state vector (position, velocity, attitude) over time by means of sensors.
- *Guidance*, refers to the determination of the desired trajectory from the current SCE's position to the target. Guidance plays the role of the system's controller, deciding which actions should be taken to change the vehicle's state vector over time in a proper manner.
- *Control*, plays the role of the system's actuator, manipulating the forces needed to execute the guidance commands.

A. GNC System Design

To perform the TAG sampling chain validation, the SCE must follow a precise sequence of steps. Therefore, it was required to control the three testbed's DoFs. The SCE must approach the target following a predetermined trajectory and with the proper speed. For this reason, it was required a position control on both transversal and rotational motions, and a speed control on longitudinal motion.

The next step was determining if a fully or partially autonomous GNC system was needed. First, the target is about 8 times smaller than testbed, meaning that a high positioning precision is required. Moreover, the front plate of the sampling tool is about 4 meters away with respect to the SCE's body center, so also small rotations mean high deviations at the tip of the sampling tool. The implementation of a remote control would then be impractical, also due to safety reasons. In fact, all personnel must maintain a safe distance during the test, so the operator may not be able to clearly see the testbed and its relative position with respect to the target. On the other hand, the operator should control all three SCE's DoFs, with a high workload, and a long training required to perform the test in the right way. The short time available to complete the SCE's design, fabrication, and test, brought to the selection of a fully autonomous GNC system.

1. Navigation

The purpose of the Navigation part of the GNC system is the determination of the SCE's state vector (position, velocity and attitude) with respect to the target. This information is used to determine the actions needed to carry the SCE from the current position to the target, following a predetermined trajectory.

JPL commonly utilizes motion capture (mocap) systems to track objects. The mocap system adopted was provided by Vicon®, and is based on an optical-passive approach, which utilizes retroreflective passive markers placed on the object to track, and tracked by infrared cameras.

Tracking the SCE's position requires only a single marker placed in the center of the SCE's body. On the other hand, to determine the SCE's orientation, at least two markers are required. The Vicon® software makes possible to define the so called Vicon® objects. These virtual objects are user-defined groups of at least two markers considered by the Vicon® system as single objects with a centroid and an orientation. Applying this concept to the SCE, it should be theoretically possible determining its orientation by simply creating a Vicon® object made of two markers. This solution does not actually work

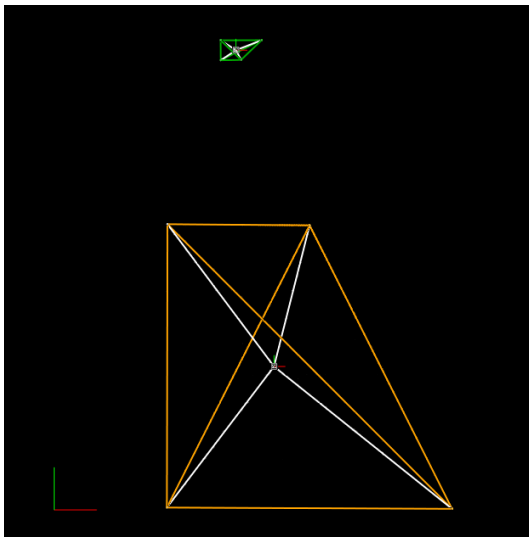

Figure 2. Vicon® objects representing the SCE (orange) and the target (green).

because a Vicon® object made of two markers is a straight line, which is symmetric, so its reference frame is not uniquely determined. The worst consequence is that the reference frame can randomly flip, making unreliable the evaluation of the object's orientation. The Vicon® object must then be asymmetric, so at least three markers are needed. The goal is to carry the sampling tool exactly in the right position and orientation with respect to the target, so the position of the BiBlade's front plate is the actual information needed, instead of the position of the SCE's body. Since placing a marker directly on the BiBlade was not feasible, a marker was placed on the SCE's body, aligned with the BiBlade. A user-defined correction was then applied to obtain the actual BiBlade's front plate position. For a better reliability, a four-markers object was created. Three markers were placed at the corners of the SCE's body. The fourth marker is the *BiBlade marker*, and it is aligned with the BiBlade's front plate position. The object's centroid lies at the crossing point of the white lines, as showed in Fig. 2. At the centroid level is defined also the reference frame of the object. It should be noted that the reference frame of the object is required to determine the orientation of the Vicon® object only, since the BiBlade's position is determined by using the dedicated *BiBlade marker*.

The same procedure was applied to create the Vicon® object for the target to determine the relative position between the BiBlade and the target. Also in this case, the object is made of four markers. Three of them was placed at the corners of the simulant box. The fourth marker, called *target marker*, makes the object asymmetric, and lies at the level of the simulant surface, aligned with the center of the box.

Once the Vicon® objects are defined, the Vicon® software can provide information about markers position and objects' orientation with respect to a global reference frame defined by using a calibration sequence.

The velocity of the SCE was calculated by knowing the markers' position and the sampling time of the Vicon® system.

$$V = \frac{(Y_{V_{t-1}} - Y_{V_t})}{t} \tag{1}$$

- t is the sampling time, equal to 1 sec. The value selected is a trade-off between the time resolution and the amount of data sent to the SCE's onboard computer to perform the GNC duties. The typical sampling frequency of the Vicon system is 100 Hz. By the way, a too high value brings to delays because of process queues. On the other hand, the SCE is low enough to keep the sampling frequency at 1 Hz. This value highly reduces the risk of delays and gives a good time resolution.
- Y_{V_t} is the Y_V position at time t.
- $Y_{V_{t-1}}$ is the Y_V position at time $t-1$.

All the elements needed to define the state vector of the SCE was then defined by using the notation of Eq. (2).

$$S = \{R, A_V, V\} = \{[X_V, Y_V], A_V, V\} \tag{2}$$

- R represents the relative position along X-axis and Y-axis, $[X_V, Y_V]$.
- A_V represents the relative attitude.
- V represents the relative velocity.

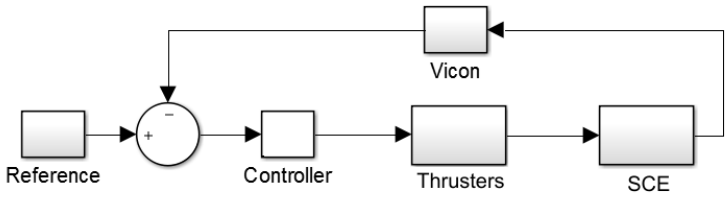

Figure 3. Control system's block diagram.

2. Guidance

Once the state vector is defined, the GNC system determines the guidance commands that should be executed to carry the SCE from the current position to the target, following the desired trajectory. Since the purpose of the SCE is the validation of the TAG sampling chain, the test conditions must be controllable, so predetermined trajectories were defined. Four trajectories were considered to cover the main mission scenarios. These trajectories were defined by imposing constraints on SCE's DoFs. These constraints become guidance commands to achieve the desired goal.

- *Trajectory 1*, is the simplest path. The SCE must follow a straight line, aligned with the center of the target. The SCE approaches the target perpendicularly with a null attitude angle. The mathematical constraints for this path follows.
    - $X_R = 0$, the BiBlade must approach the target perpendicularly.
    - $Y_R = NC$, this variable is Not Constrained (NC) because it is not strictly involved in the trajectory definition. It is relevant for other purposes such as the determination of the SCE' relative velocity, and for the autonomous triggering system of the sampling process.
    - $A_R = 0$, the SCE's attitude angle must be null.
    - $V = V_R$, the velocity is already constrained to a predefined value by test requirements.
- *Trajectory 2*, is similar to the previous one. The SCE still approaches the target perpendicularly, but with a not null attitude angle. The purpose is to test the BiBlade sampling capabilities in case of angled approach while SCE's velocity vector is still perpendicular to the target.
    - $X_R = 0$
    - $Y_R = NC$
    - $A_R = \beta$, the BiBlade approaches the target with two different attitude angles, 30° and 45°.
    - $V = V_R$
- *Trajectory 3*, this trajectory is not perpendicular to the target anymore. The approaching path is angled, and the SCE's attitude angle is null.
    - $X_R = Y_V \tan\beta$, the X-position of the SCE is constrained by the requirement to follow an angled approaching path. The X-position must have a precise value which depends on the current Y-position and on the approaching angle β = [30°, 45°]. The purpose is to test the BiBlade sampling capabilities in case of relative motion along X-axis between the SCE and the target.
    - $Y_R = NC$
    - $A_R = 0$, the approaching path only must be angled, the SCE's attitude angle must be null.
    - $V = V_R$
- *Trajectory 4*, this trajectory is similar to the previous one. The SCE still approaches the target with an angled path, but with a not null attitude angle. The purpose is to test the BiBlade sampling capabilities in case of relative motion along X-axis between the SCE and the target, with a not null attitude angle.
    - $X_R = Y_V \tan\beta$
    - $Y_R = NC$
    - $A_R = \beta$
    - $V = V_R$

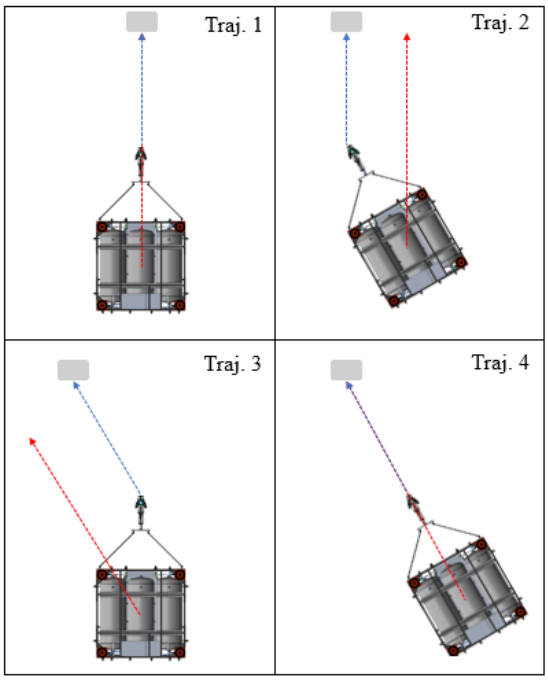

Figure 4. TAG trajectories. BiBlade trajectories (blue), and SCE's body trajectories (red).

3. Control

This part of the GNC system compares the desired output (coming from Guidance) with the actual output (coming from Navigation) to determine the command signals for the actuators (i.e. the air thrusters), thus enabling the physical control of the SCE. The longitudinal motion requires a velocity control, since it must keep the SCE's velocity at the predefined value with a precision of ±0.5 cm/s. On the other hand, the rotational and transversal motions require a position control. The rotational control must have a precision of ±0.01°, while the transversal control must have a precision of ±1 cm. The control logic largely depends on the features of the actuators selected. On/off valves require the Pulse-Width Modulation (PWM), hence a linear control was selected. PWM technique encodes the continuous control signal coming from the controller into a pulsing signal. The PWM output is a rectangular wave which assumes the value of 0 when the valve is completely closed, and the value of 1 when the valve is completely open. The PWM signal is directly applicable to control the thrusters since it is made of pulses which command to open or close the thrusters' solenoid valves. The PWM signal has a constant period and a variable duty cycle, which is the fraction of one period during which the signal equals 1. A PWM signal can be generated by using the intersective method, which requires to compare a reference signal and a modulation waveform, which is typically a sawtooth or a triangular waveform [10,11].

Since the SCE is controlled by means of air thrusters, the information needed is the amount of thrust that each thruster must provide to move the SCE to comply with the guidance commands. The thrust function, which represents the reference signal, derives by the mathematical model of the system's physics.

Applying the Newton's second law of motion, the SCE's dynamics is represented by Eq. (3).

$$F_I + F_A + F_G = T \tag{3}$$

$$M\ddot{x} + K_A\dot{x} + F_G = T \tag{4}$$

$$\ddot{x} = \frac{(T - K_A\dot{x} - F_G)}{M} \tag{5}$$

- F_I is the SCE's force of inertia.
- F_A is the friction force.
- F_G is the gravity force due to not-flatness of the floor, experimentally measured [8].
- T is the thrust.
- M is the SCE's mass.
- K_A is the friction coefficient, experimentally measured [8].
- $\dot{x}$ and $\ddot{x}$ are respectively the SCE's velocity and acceleration.

A widely used controller is the PID (Proportional-Integral-Derivative). This controller continuously evaluates the error $e(t)$ between a setpoint and the measured value of a process variable, and applies a correction based on proportional, integral, and derivative terms, called gains. The controller tries to reduce the error over time by producing an output called control variable, which is a command for the actuators. In the present case, the control variable is the thrust that the air thrusters must provide to move the SCE according to the guidance commands. The control variable is calculated by a weighted sum [10,11].

$$T(t) = K_P\, e(t) + K_I \int_0^t e(\tau)\, d\tau + K_D\, \frac{de(t)}{dt} \tag{6}$$

The proportional term produces an output signal which is proportional to the error. The integral term is proportional to the integral of the error, hence it is proportional to the summation of the past values of the error. This term enables to cancel the steady-state error, since the integral of the error will accumulate over time. If the saturation of the controller output occurs, the integral action continues to sum the error, hence the integral term continuously rises, demanding for ever greater control action. This phenomenon is called windup and can be solved by using anti-windup systems, such as back calculation, integral term bounds, etc. The derivative term is proportional to the derivative of the error; hence it is proportional to the error rate of change, accounting for possible future trends of the error. This term could bring to the saturation of the controller output in case of high rate changes in the error [10,11].

The design practice adopted was starting with a pure proportional controller. Adding too much terms is often not necessary, and could bring to a uselessly complex controller, which would be also more difficult to be tuned, debugged, and tested. Simulations and results showed that a pure proportional controller was satisfactory to achieve the desired goals.

Since a position control is needed for the transversal DoF, the actual SCE's transversal position X_V, measured by the Vicon® system, must be compared with the desired transversal position X_R, derived from the guidance commands. The thrust needed for transversal control is then the derived error $e(t)$ times the proportional gain K_{P_T}.

$$T(t) = K_{P_T}\, e(t) = K_{P_T}\, (X_V - X_R) \tag{7}$$

The built-in Simulink's Controller Tuner was used to perform a preliminary tuning of the controller, along with the analysis of the step response. The results showed a good preliminary setup. The gain of the controller, set at a value of K_{P_T} = 5000, makes the step response fast and deep. This is particularly important to keep the position within a reasonably narrow band to avoid excessive deviations with respect to the target.

Hardware-in-the-loop (HIL) tests were conducted to refine the tuning. Controller performances were improved considering the slight deviations between the mathematical model and the reality, mainly due to uncertainties on friction and not-flatness of the floor. The gain was raised to K_{P_T} = 5500, differing with respect to the preliminary one by just 10%, and confirming the goodness of the mathematical model. The rise time of 1.55 seconds is short enough to guarantee a fast response. The settling time of 3.84 seconds guarantees a transversal velocity at a low position error which is comparable with the longitudinal velocity, whereas it increases as the error increases. This is particularly important in terms of system reactivity. Finally, the overshoot at 2.71% makes the control system damped enough to avoid any further oscillation.

Once the thrust function over time is defined, it is possible to convert the continuous function $T(t)$ into a discrete, rectangular function by using the PWM method. Since the thrusters' on/off valves can be completely open or completely closed only, they can provide zero or full thrust only. The control was then achieved by varying the duty cycle of the PWM signal. The sum of the impulses J_n given by the m PWM pulses, equals the impulse J_C of the function $T(t)$.

$$J_C = \int_{t_1}^{t_2} T(t)\, dt = \sum_{n=1}^{m} J_n \tag{8}$$

The modulation signal is characterized by an amplitude and a frequency. The amplitude must be equal to the maximum thrust deliverable by the thrusters, and was set by properly coding the control system. Since the modulation signal is generated by a single equipment, the frequency selected must be adopted for all controls. A frequency adequate for all controls was the selected by considering also the Nyquist-Shannon sampling theorem. Since the frequency of the reference signal of all controls ranges from 0.4 Hz to 1 Hz, a modulation frequency of 5 Hz was selected to guarantee a good sampling of the signal in every case.

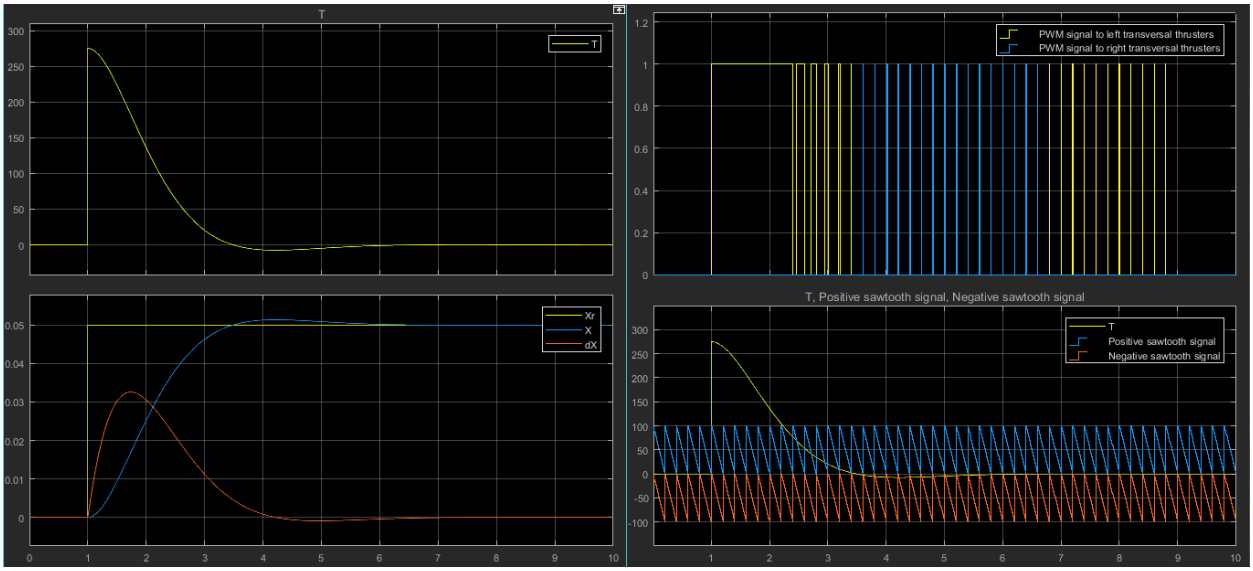

Figure 5. Bottom left: transversal controller step response. Reference position (Xr), actual position (X), speed (dX). Top left: thrust function for transversal control (T). Bottom right: thrust function and sawtooth signal. Top right: PWM signal for transversal control.

The bottom right part of Figure 5 shows the case of thrusters' oversaturation. This happens if the thrust required to perform the control exceeds the maximum thrust deliverable by the thrusters. For this reason, the PWM signal remains in the high state until error on position is small enough to keep the thrust required within the limit.

The rotational control shares the controller setup of the transversal one, since both require a position control with the same features of responsivity. HIL tests confirmed this choice.

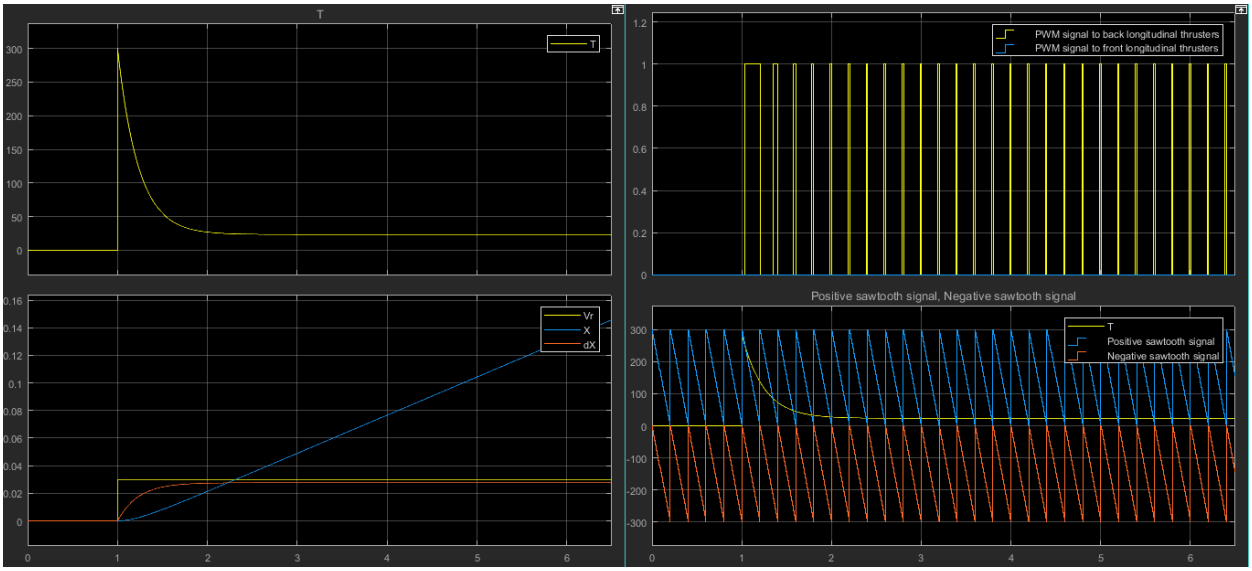

Figure 6. Bottom left: longitudinal controller step response. Reference speed (Vr), actual speed (dX), position (X). Top left: thrust function for longitudinal control (T). Bottom right: thrust function and sawtooth signal. Top right: PWM signal for longitudinal control.

Since a velocity control is needed for the longitudinal DoF, the actual SCE's velocity V_V, measured by using the Vicon® data, must be compared with the desired velocity V_R, coming from the requirements. The thrust needed for longitudinal control is then the derived error $e(t)$ times the proportional gain K_{P_L}.

$$T(t) = K_{P_L}\, e(t) = K_{P_L}\,(V_V - V_R) \tag{9}$$

A preliminary gain value of K_{P_L} = 10000 was determined by using the Simulink's Controller Tuner. Since a continuous motion at a defined velocity is needed, a constant output from controller is required. An error between the desired speed and the actual speed then must be constantly maintained. The steady state error produces the thrust required to overcome the friction forces, keeping the SCE's velocity at a constant value. HIL tests were conducted also in this case to refine the tuning of controller. The updated gain of K_{P_L} = 9500 differs with respect to the preliminary one by 5%, confirming the goodness of the mathematical model.

B. GNC System Implementation

The drivers for GNC system implementation considered the need to realize a full off-the-grid testbed, in terms of both data and power. The system is composed by two main parts communicating wirelessly; the Ground Station (GS) and the On-Board-Station (OBS), which is placed on the SCE. The purpose of the GS is to gather data from the Vicon® system, manage them, and send navigation information to the OBS. The purpose of the OBS is to receive navigation data from the GS, manage them, and send control commands to the SCE's actuators.

1. Ground Station

Since the main purpose of the GS is to gather data from the Vicon® system and send them to the OBS, the Vicon® computer (VC) is the first block of the system, since it is the interface between the Vicon® cameras and the user. The VC is connected to the Control Station (CS), which is the interface between the operator and the testbed. The CS is an Intel® NUC running Linux Ubuntu. An application, called Control Station's Software (CSS), was developed to monitor the test, having the capability to start/stop it. Furthermore, the CSS automatically takes data from the VC, creates the data packages containing the navigation information, and sends them to the OBS.

As said before, the CS has the capability to start/stop, and monitor the test. This is achieved by sending commands via the CSS's Graphical User Interface (GUI). These commands activate specific subroutines of the GNC software that runs on the OBS. To realize a full off-the-grid testbed, the GS communicates with the OBS via wireless link. Two routers, the first one on the GS and the second one onboard the testbed, was used for this purpose.

2. On Board Station

The first two blocks of the OBS are the router that receives the information sent by the GS, and an Intel® NUC that manages them. The NUC runs a simple code that reads the data coming from the router and retransmits them to an Arduino Due development board, which runs the GNC software. The main advantage of using a development board is the possibility to directly connect I/O devices, making simple and fast the embedded systems prototyping and testing. Another input to the Arduino board is the Function Generator (FG), used to generate the modulation signal for the PWM. A relay module is finally used to transmit the PWM signals to the thrusters' valves.

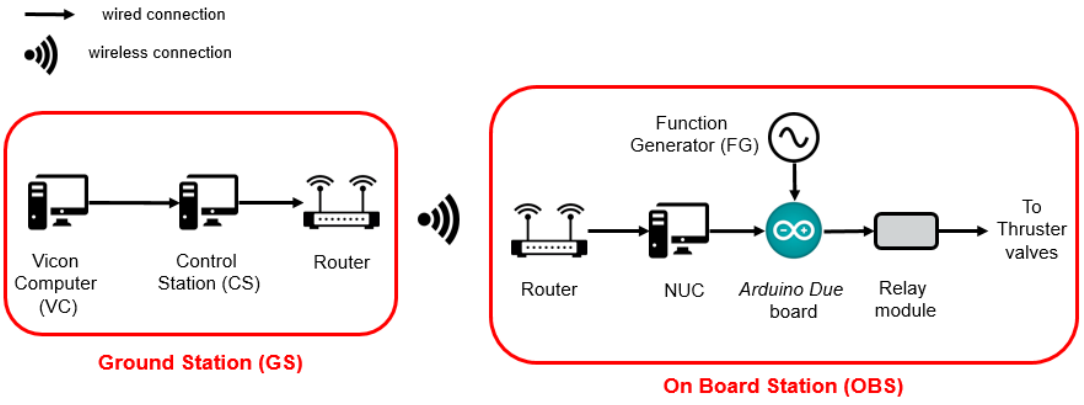

Figure 7. GNC hardware architecture.

IV. Electric Power System

The EPS architecture typically consists of two main subsystems [9].

- Primary EPS, which generates electrical power from the primary energy source, stores the electrical energy, and distributes it to the main electrical buses.
- Secondary EPS, which distributes the electrical power, properly regulated, to the final users.

Since the goal was to realize a full off-the-grid system, the power source was placed onboard the SCE, without any kind of umbilical connection with the environment. Li-ion batteries were identified as the best power source for this

purpose. There were some high-level requirements characterizing the EPS; the power budget, the power profile, and the working time. The working time is related with the maximum expected duration of the test, which is about six minutes.

Whereas all other equipment have a constant power consumption, the BiBlade power needs varies over the test. The BiBlade absorbs 240 W in *waiting mode*, which is the mode that precedes the sampling process. The power needed rises to 960 W in *firing mode*, when the blades of the sampling tool are retracted to be fired into the target. The power needs of the SCE testbed then vary from 762 W with the BiBlade in *waiting mode*, to 1482 W with the BiBlade in *firing mode*. Excluding the BiBlade, the power budget suggested to consider a main bus at the voltage of the main load, which is represented by the sixteen solenoid valves adopted for the thrusters and the air bearings. A series of voltage regulators and DC-DC converters were used to transform the voltage of the main bus into the voltage required by the other loads. Finally, some countermeasures were implemented for safety reasons. Eight wired e-stops were directly applied to the SCE testbed, whereas a wireless e-stop was used to remotely shut down the testbed in case of emergency.

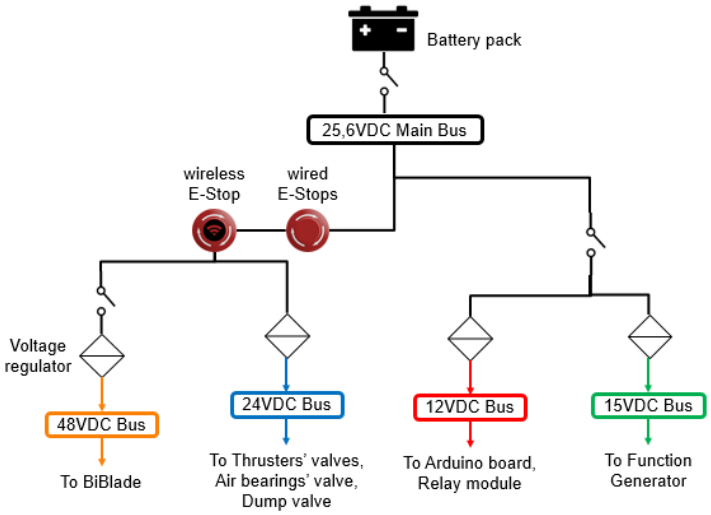

Figure 8. EPS architecture.

V. Conclusion

The full-scale SCE testbed was designed and fabricated to enable end-to-end validation of TAG sampling, sample measurement, and sample transfer to a representative Sample Return Capsule (SRC). Each of these capabilities was validated using specific testbeds. The SCE enabled the end-to-end integrated validation using a single testbed, making the results more realistic.

Tests helped to better understand the sampling dynamics and its effects on SC behavior. Validation results showed the goodness of SCE design and implementation, confirming that the sampling tool is very robust for sampling in Comet Surface Sample Return mission scenarios. For the initial tests, the BiBlade sampling tool was directly mounted on the SCE in a way that is representative of the mounting stiffness that will be potentially realized for the mission. Future developments will include a robotic arm to deploy the sampling tool and a SRC to deposit the samples.

Tests performed represented the first attempt to use a full-scale/mass SCE to reproduce the SC operations in a two-dimensional (2D), low-friction plane. Previously, only scaled testbeds have been used to perform this task [12,13]. The main advantage of a full-scale/mass SCE is the opportunity to study the SC dynamics in a more realistic fashion, reproducing mission-like features like masses, inertias, forces, reactions, and global SC response. The SCE was not designed for a specific, high precision floor, making it suitable to be used on common building floors. Moreover, the SCE was designed to be autonomous in terms of both power and controls, making easier the management of the test. The modular design of both power and control systems makes the SCE flexible enough to be easily adapted to several applications with different needs, being programmable to perform a wide variety of tasks, as well as able to vary its power output.

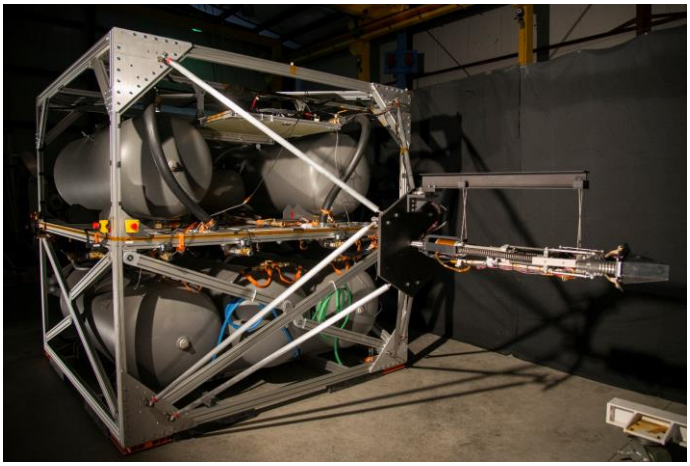

Figure 9. Spacecraft Emulator (SCE) testbed.

Acknowledgments

This research was carried out at the Jet Propulsion Laboratory, California Institute of Technology, and was sponsored by the JPL Visiting Student Researchers Program and the National Aeronautics and Space Administration.

References

[1]Committee on the Planetary Science Decadal Survey, "Vision and Voyages for Planetary Science in the Decade 2013-2022," National Research Council, The National Academies Press, 2011.

[2]Fountain, G. H., et al., "Comet Surface Sample Mission Study," SDO-11998, prepared for NASA's Planetary Science Division, April 30, 2008.

[3]Backes, P., et al., "Experimental Results with the BiBlade Sampling Chain for Comet Surface Sampling," *IEEE Aerospace Conference*, Big Sky, Montana, March 5-12, 2016.

[4]Backes, P., et. al., "Sampling System Concepts for a Touch-and-Go Architecture Comet Surface Sample Return Mission," *AIAA Space Conference and Exposition*, San Diego, California, August 4-7, 2014.

[5]Backes, P., et. al., "BiBlade Sampling Tool Validation for Comet Surface Environments," *IEEE Aerospace Conference*, Big Sky, Montana, March 4-11, 2017.

[6]NewWay Air Bearings, "Air bearings application and design guide," 50 McDonald Blvd. Aston, PA 19014, 2006.

[7]AeroGo, Inc., "Floor Surface Specification, concrete floors," 1170 Andover Park West, Seattle, WA 98188, 2001.

[8]Mongelli, M., *Full-scale spacecraft simulator design for a 2D zero gravity small body surface sampling validation*, Master's thesis, Mechanical and Aerospace Dept., Politecnico di Torino, Italy, 2016.

[9]Corpino, S., "Aerospace Systems", Politecnico di Torino, Torino, Italy, 2015 (unpublished).

[10]Maggiore, P., "Onboard Aerospace Systems", Politecnico di Torino, Torino, Italy, 2013 (unpublished).

[11]Maggiore, P., "Modelling, Simulation and Experimentation of Aerospace Systems", Politecnico di Torino, Torino, Italy, 2015 (unpublished).

[12]Schwartz, J. L., Peck, M. A., Hall, C. D., "Historical review of air-bearing spacecraft simulators," *Journal of Guidance, Control, and Dynamics*, Vol. 26, No. 4, July-August 2003.

[13]Barnhart, D., Barrett, T., Sachs, J., Will, P., "Development and operation of a micro-satellite dynamic test facility for distributed," *AIAA Space Conference and Exposition*, Pasadena, California, September 14-17, 2009.